Research Article

Numerical and Analytical Investigation of Free Vibration Behavior of Porous Functionally Graded Sandwich Plates

Emad Kadum Njim [a] , **Mohammed Hamza Al-Maamori** [b] , **Royal Madan** [*c] ,
Sadeq Hussein Bakhy [d] , **Muhannad Al-Waily** [e] , **Pallavi Khobragade** [f],
Lazreg Hadji [g]

[a] *Ministry of Industry and Minerals, State Company for Rubber and Tires Industries, Najaf, Iraq*

[b] *Prosthetics & Orthotics Eng. Department, College of Engineering, AL-Mustaqbal University, 51001 Hillah, Babil, Iraq*

[c] *Department of Mechanical Engineering, Graphic Era (Deemed to be University), Dehradun, 248002, Uttarakhand, India*

[d] *University of Technology, Mechanical Engineering Department, Baghdad, Iraq*

[e] *University of Kufa, Faculty of Engineering, Mechanical Engineering Department, Najaf, Iraq*

[f] *Department of Civil Engineering, Dev Bhoomi Uttarakhand University, Dehradun, India*

[g] *Department of Civil Engineering, University of Tiaret, Tiaret, 00213, Algeria*

ARTICLE INFO

ABSTRACT

This study investigates the free vibration analysis of a sandwich plate made of functionally graded materials (FGMs) with porosities to evaluate the natural frequency. Five parameters contribute to FGM: porous index, elastic parameters, porosity ratio, length-to-thickness ratio, and length-to-width ratio. Taking into account the thickness of the FGM plate, it is assumed that the plate has a new distribution of porosities. An investigation based on classical plate theory (CPT) examines kinematic relationships. This paper presents results for metal-ceramic functionally graded rectangular plates with a power law through the variation of volume fractions with porous ratio. A margin of error of not more than 5% applies to thin and thick plates. To validate the analytical results, a numerical investigation was conducted by employing the finite element method using ANSYS. This investigation was conducted on a 3D model of an FG system with SOLID186 an eight-noded element. Using various boundary conditions and selected models, illustrated the influence of porosity distribution characteristics on sandwich plate dynamic response. It was found that the frequency parameter of the plate increases with the increase in the sandwich structure mounting constraints. The plate thickness was divided into N layers to show the effect of several layers on the obtained results. It was found that the natural frequency for the FGM sandwich plate remains the same regardless of the number of layers for the same FGM thickness.

1. Introduction

The functionally graded materials (FGMs) are a class of composite that continuously varies material properties directionally, thereby eliminating stress concentrations [1]. The change in composition can be unidirectional, bidirectional, or multi-directional depending on

---

* Corresponding author.

E-mail address: royalmadan6293@gmail.com

the applications [2, 3]. The FGM fabricated are either stepped-wise or continuously graded along the defined directions. There are several manufacturing techniques available which are categorized as solid-based, liquid-based, and gas-based [4]. FGM plates may suffer from porosities and micro-voids during fabrication, which may compromise their strength [5]. Sandwich structures because of their low weight and high stiffness generate higher natural frequency and so have vast industrial applications [6]. It consists of a lightweight core that gives damping and energy absorption properties bonded by face sheets at the top and bottom [7]. Many researchers have analyzed the behavior of sandwich structures by performing various analysis such as free vibration [8], impact [9], and buckling [10], to name a few.

Bending analysis of the FG sandwich beam made up of isotropic core and FG skins was performed using shear deformation theory. They demonstrated that the impact of indices is less in softcore as compared to hardcore [11]. The penalty method was employed to investigate the free vibration behaviour of the FG core and its results are compared with isotropic materials. The problem of the FG beam was then solved under various boundary conditions. The accuracy of the proposed meshless method was verified with finite element analysis [12]. Buckling analysis of a sandwich plate composed of FG skin and isotropic core for different boundary conditions was performed in which an all-clamped boundary condition yielded the highest buckling load [10]. Buckling analysis of the FG sandwich plate under thermo-mechanical loading was performed using Navier's method. The analysis was performed considering two cases: FG skin and isotropic core and FG core with isotropic skin [13]. Moreover, for similar cases, buckling analysis was performed using the refined finite strip method and found sandwich plates with homogenous face sheets and FG core produce larger central deflection [14]. For hard core bending and buckling analysis of FG circular plate was performed using revised Reissner's theory. Out of various boundary conditions studied simply supported boundary conditions produce maximum deflection and fixed-end supported boundary conditions develop minimum [15].

Free vibration of porous FG sandwich beam was performed using the finite element method. A comparative analysis was conducted considering both hard core and soft core and the effect of grading indices on natural frequency was seen. It was found that the impact of material tailoring is more significant in softcore than hardcore [16]. The free vibration analysis of functionally graded plates with porosity

composed of a mixture of Aluminium (Al) and Alumina (Al_2O_3) embedded in an elastic medium using a novel mathematical formulation was studied [17]. Investigated the influences of material property distribution and porosity impact on the FG sandwich plate natural frequencies based on different boundary conditions [18]. Investigated functionally graded porous plates reinforced by graphene platelets to determine their free vibration and stability [19]. The free vibration of the FG core sandwich beam problem was solved using the complementary functions method. The effect of different gradation types on the natural frequency was seen and the parameter was minimum for exponential graded core than power law gradation [20]. Numerous methods have been so far introduced in investigating the behavior of sandwich structures such as the finite element method [21], Navier's solution [22], Galerkin Vlasov's method [23], differential quadrature finite element method [24], high-order shear deformation theory [19, 25], boundary finite element method [26], Asymptotic Numerical Method [27], meshless methods [28–30], collocation method [31], and iso-geometric approach [32].

With advancements in the manufacturing of FGMs, it is now possible to tailor properties in multiple directions by varying composition, microstructure, or porosity. The fabrication technique used can be categorized as solid-based, liquid-based, and gas-based methods [33, 34]. In one study, a powder metallurgy method was used to fabricate a layered FG disk by varying the volume fraction across the layers. The study revealed that sintering temperature, compaction load, and reinforcement particle shape play crucial roles in the occurrence of porosity [35, 36]. A FGM with multiple layers can be fabricated by the use of an additive manufacturing method [37,38]. However, in this technique also some challenges include melting, molten pool flow, crystallization, etc., influencing the product density [39].

To achieve continuous gradation of material properties methods such as a direct ink writing technique [40] and centrifugal casting can be used [41–43]. While porosity can be minimized, the careful selection of processes and parameters is essential for developing a dense product. Since porosity significantly impacts the performance of FG structures, a comparison of FG sandwich beams with and without porosity was conducted through bending and free vibration analysis [44, 45]. The distribution of porosity can be either even or uneven in both homogeneous structures and functionally graded materials (FGMs). Additionally, when analyzing nanostructures, such as plates or

beams, the distribution of porosity is also taken into account [46].

The free vibration analysis of a functionally graded (FG) sandwich plate under various boundary conditions was conducted using Hamilton's principle. In this study, the face sheets of the sandwich plate are composed of FGM, while the core is made of an isotropic material. It was observed that porosity significantly impacts beams with a high side-to-thickness ratio. Among the boundary conditions considered, the clamped-clamped (FCFC) condition resulted in the maximum frequency, while the simply supported (SSSS) condition yielded the minimum frequency [47].

The purpose of this study is to provide a mathematical model and exact solution for determining the natural frequency of the FG sandwich plate. The free vibration of a rectangular sandwich plate containing functionally graded porous metal bearing power law material gradation was considered. Parametric investigation on the sandwich structure was investigated by understanding the impact of porous index, elastic parameters, porosity ratio, and length-to-thickness ratio.

In the current investigation, it was assumed that the plate material varies smoothly along its thickness. Furthermore, the analysis was extended for different boundary conditions namely CCCC, CCCS, FCFC, CSCS, and SSSS boundary conditions. The accuracy of the present methodology was verified with numerous methods published in the literature.

2. Mathematical Formulations

The FGM plate used in this study was made from ceramic metal. Plate dimensions a, b, and h indicate length, width, and thickness, respectively. Initially, it is assumed that the top surface of the tape (z = h/2) has a material structure that is ceramic-rich and continually varies from the bottom surface, which is metal-rich.

To describe the plate's motion, the middle surface is given a cartesian coordinate system (x, y, z) in which x and y represent the plate's in-plane coordinates, and z is the plate's out-of-plane coordinates.

Figure 1 shows the geometrical description of the imperfect FGM plate. Since the effects of Poisson's ratio variation on FG plates' response are minimal, it is assumed to be constant for convenience [48]. Classical plate theory (CPT) gives stress-strain relations [49].

$$\sigma_{xx} = \frac{E}{1 - v^2}(\varepsilon_{xx} + v\varepsilon_{yy})$$

$$\sigma_{yy} = \frac{E}{1 - v^2}(\varepsilon_{yy} + v\varepsilon_{xx}) \tag{1}$$

$$\sigma_{xy} = G\gamma_{xy} = \frac{E}{2(1 + v)}\gamma_{xy}$$

A plate element's linear constitutive relations, such as its bending and twisting moments. In the case of pure bending, the equation can be written as follows:

$$M_{xx} = \int_{-\frac{h}{2}}^{\frac{h}{2}} \sigma_{xx}zdz = -D\left(\frac{\partial^2 w}{\partial x^2} + v\frac{\partial^2 w}{\partial y^2}\right)$$

$$M_{yy} = \int_{-\frac{h}{2}}^{\frac{h}{2}} \sigma_{yy}zdz = -D\left(v\frac{\partial^2 w}{\partial x^2} + \frac{\partial^2 w}{\partial y^2}\right) \tag{2}$$

$$M_{xy} = \int_{-\frac{h}{2}}^{\frac{h}{2}} \sigma_{xy}zdz = -(1 - v)D\frac{\partial^2 w}{\partial x \partial y}$$

where D rigidity parameter of the plate,

$$D = \frac{Eh^3}{12(1 - v^2)} \tag{3}$$

Alternatively, the second-order equilibrium equation in Kirchhoff plate theory can be expressed as follows:

$$\frac{\partial^2 M_{xx}}{\partial x^2} - 2\frac{\partial^2 M_{xy}}{\partial x \partial y} + \frac{\partial^2 M_{yy}}{\partial y^2} = I_o\frac{\partial^2 w}{\partial t^2} \tag{4}$$

In Eq. 4, replace bending and twisting moments with equivalent expressions. The equilibrium can be expressed in terms of deflections (w) of the plate as follows:

$$D_f\left(\frac{\partial^4 w}{\partial x^4} + 2\frac{\partial^4 w}{\partial x^2 \partial y^2} + \frac{\partial^4 w}{\partial y^4}\right) + I_o\frac{\partial^2 w}{\partial t^2} = 0 \tag{5}$$

where, D_f is the flexural rigidity of the FG plate and I_o is the inertial coefficient.
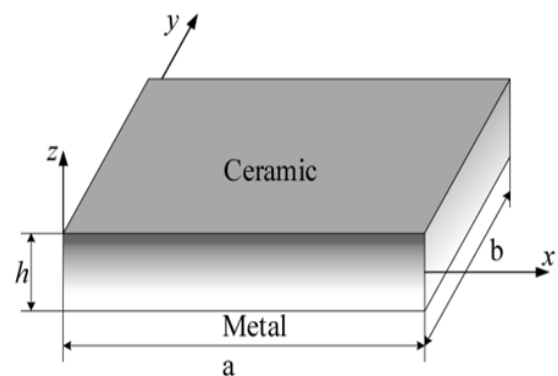

Fig. 1. FGM Plate

### 2.1. Mathematical Modeling of Rectangular FGM Plates

It is generally possible to interpret continuous variations in material properties of FG plate constituents using an exponential law, sigmoid law, or power-law interpretation. Assuming the power-law variation in FG plates, we can define ceramic volume fraction (V_c) as follows:

$$V_c(z) = \left(\frac{z + \frac{h}{2}}{h} \right)^k \tag{6a}$$

The total volume fraction of FGM is the sum of metal and ceramic compositions and is stated as:

$$V_m(z) + V_c(z) = 1 \tag{6b}$$

The metal volume fractions are represented by (V_m), and (k) is the power-law variation index which ranges from $[0, \infty]$. Assigning a value of $k = 0$ defines pure ceramic, whereas assigning a value of $k = \infty$ indicates pure metal.
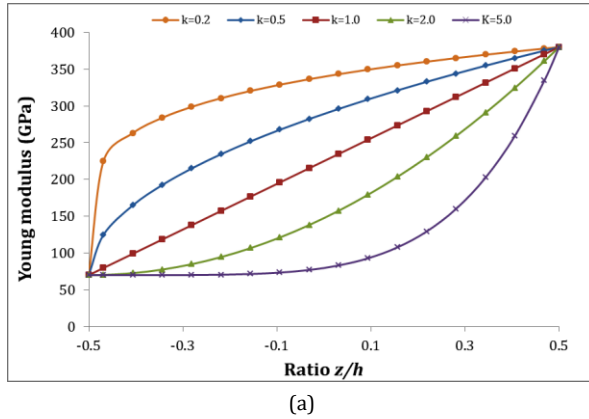
There is an assumption that the top surface's material structure (z=h/2) varies continuously from the bottom surface's metal-rich surface (z = h/2). To describe the plate motion, the cartesian coordinate system (x, y, z) is used, with x and y representing in-plane coordinates and z denoting out-of-plane coordinates. The gradation variation along the FGM can be written as:

$$\emptyset(z) = (\emptyset_c - \emptyset_m) \left(\frac{z + \frac{h}{2}}{h} \right)^k + \emptyset_m \tag{7}$$

In Eq. (7), $\emptyset_c$ and $\emptyset_m$ are the values of the FG plate's ceramic and metal material properties and constituents, respectively. As shown in Fig. 1, there are variations in materials properties. Based on the results of Figure 2, it is shown that material properties obtained for the power law index are generally **k** = 0.22, 0.55, 0.6, 1, 2, and 5. This range of values of **k** confirms the presence of both the ceramic and metal-rich mixture cases. Poisson's ratio implies a constant, while Young's modulus (E) and mass density (ρ) vary through the plate thickness.
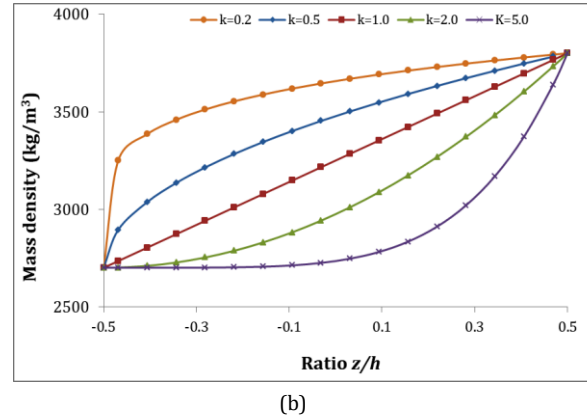

(a)

(b)

Fig. 2. Power law variation of FG (Al/Al₂O₃) (a) Elastic modulus (b) Mass density

Following is an illustration of how to derive the governing differential equations defining the free vibration of FG plates based on general classical plate theory (CPT).

$$D_{FG} = \int_{-\frac{h}{2}}^{\frac{h}{2}} \frac{z^2}{(1 - v_f^2)} E(z) dz$$

D_{FG} is the flexural rigidity of the plate,

$$D_{FG} = \frac{(E_c - E_m)h^3}{(1 - v_{FG}^2)} \times$$

$$\left\{ \frac{1}{k+3} - \frac{1}{k+2} + \frac{1}{4(k+1)} \right\} + \frac{E_m h^3}{12(1 - v_{FG}^2)} \tag{8}$$

and,

$$I_o = \int_{-\frac{h}{2}}^{\frac{h}{2}} \rho(z) dz \tag{9a}$$

According to the volume fraction index, the FGM plate's inertial coefficient I_o is:

$$I_o = \int_{-\frac{h}{2}}^{\frac{h}{2}} \left((\rho_c - \rho_m) \left(\frac{z}{h} + \frac{1}{2} \right)^k + \rho_m \right) dz$$

$$= \int_{-\frac{h}{2}}^{\frac{h}{2}} \left((\rho_c - \rho_m) \left(\frac{z}{h} + \frac{1}{2} \right)^k \right) dz + \tag{9b}$$

$$\int_{-\frac{h}{2}}^{\frac{h}{2}} \rho_m dz \frac{(\rho_c - \rho_m)h}{(k+1)} + \rho_m h$$

where E_c and E_m are the Young modulus of a ceramic and metal material considered for analysis. The term h measures the thickness of the plate. Solving the equation the following form was then obtained:

$$
\begin{pmatrix}
\dfrac{(E_c - E_m)h^3}{(1 - v_{FG}^2)}\left(\dfrac{1}{(k+3)} - \dfrac{1}{(k+2)} + \dfrac{1}{4(k+1)}\right) \\
+ \\
\dfrac{E_m h^3}{12(1 - v_{FG}^2)} \\
\left(\dfrac{\partial^4 w}{\partial x^4} + 2\dfrac{\partial^4 w}{\partial x^2 \partial y^2} + \dfrac{\partial^4 w}{\partial y^4}\right) + \\
\left(\dfrac{(\rho_c - \rho_m)h}{(k+1)} + \rho_m h\right)\dfrac{\partial^2 w}{\partial t^2} = 0
\end{pmatrix}
\tag{10}
$$

To solve equation (10), the separation method can be used by assuming the function of deflection as:

$$w(x, y, t) = w(x, y).w(t) \tag{11}$$

2.2. Mathematical Model for FGM Plates with Porous

To determine how a rectangular plate of length a and width b behaves as a function of x and y directions, consider a plate whose edges satisfy the boundary conditions w = 0, $M_x = 0$ along x=0 or a, $M_y = 0$ at y=0, or b. Therefore, the governing equations can be expressed as follows [50]:

$$w(x, y) = \sin\frac{m\pi x}{a}\sin\frac{n\pi y}{b} \tag{12}$$

In the case of an FGM plate with porosity, its material characteristics are estimated to vary continuously over the thickness of the plate as determined by the power-law distribution (k), which indicates that the porosity will be distributed evenly inside the material based on its thickness. Accordingly, the variation of modulus and density of an FGM can be treated as:

$$E(z) = E_m + (E_c - E_m)\left(\frac{z}{h} + \frac{1}{2}\right)^k$$
$$-(E_c + E_m)\frac{\beta}{2} \tag{13a}$$

$$\rho(z) = \rho_m + (\rho_c - \rho_m)\left(\frac{z}{h} + \frac{1}{2}\right)^k$$
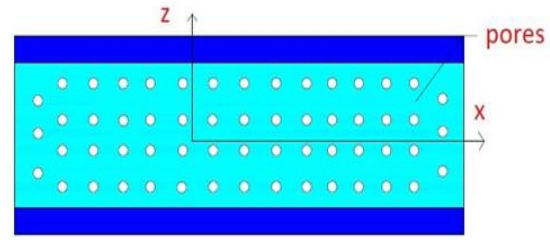$$-(\rho_c + E_m)\frac{\beta}{2} \tag{13b}$$

Fig. 3. The even porosity distribution across the core thickness

The parameter β in Eq. 13 represents the porosity fraction within the functionally graded (FG) core of the sandwich plate. This equation assumes an equal distribution of porosity between the metal and ceramic phases.

For the flexural rigidity of FG plate DFP,

$$
\begin{aligned}
D_{FP} &= \frac{1}{(1 - v_{FG}^2)}\int_{-\frac{h}{2}}^{\frac{h}{2}}\Big\{E_m + (E_c - \\
&E_m)\left(\frac{z}{h} + \frac{1}{2}\right)^k - (E_c + E_m)\frac{\beta}{2}\Big\}z^2 dz \\
&= \frac{(E_c - E_m)h^3}{(1 - v_{FG}^2)}\left\{\frac{1}{k+3} - \frac{1}{k+2} + \frac{1}{4(k+1)}\right\} \\
&+ \frac{E_m h^3}{12(1 - v_{FG}^2)} - \frac{(E_c + E_m)\beta h^3}{24(1 - v_{FG}^2)}
\end{aligned}
\tag{14}
$$

Moreover, the moment of inertia of a porosity-containing FGM plate can be expressed using its volume fraction index, which is described as follows:

$$
\begin{aligned}
I_o &= \int_{-\frac{h}{2}}^{\frac{h}{2}}\rho(z)\,dz = \int_{-\frac{h}{2}}^{\frac{h}{2}}\Big(\rho_m + (\rho_c - \\
&\rho_m)\left(\frac{z}{h} + \frac{1}{2}\right)^k - (\rho_c + \rho_m)\frac{\beta}{2}\Big)dz \\
&= \begin{pmatrix}\dfrac{(\rho_c - \rho_m)\,h}{(k+1)} + \rho_m h \\ -(\rho_c + \rho_m)\dfrac{\beta h}{2}\end{pmatrix}
\end{aligned}
\tag{15}
$$

Based on equations (10,14 and 15) and the general form of the deflection plate shown in equation (12) that meets its boundary conditions, the governing equation of the plate can be derived as described below.

The exact solution of this equation can be obtained by solving it analytically. By applying force to the solution, one can determine the plate's deflection.

$$D_f\left(\frac{\partial^4 w}{\partial x^4} + 2\frac{\partial^4 w}{\partial x^2 \cdot \partial y^2} + \frac{\partial^4 w}{\partial y^4}\right) + I_0 \frac{\partial^2 w}{\partial t^2} = 0$$

$$\begin{pmatrix} \frac{(E_c - E_m)h^3}{(1 - v_{FG}^2)}\left(\frac{1}{k+3} - \frac{1}{k+2} + \frac{1}{4(k+1)}\right) \\ + \\ \frac{E_m h^3}{12(1 - v_{FG}^2)} - \frac{(E_c + E_m)\beta h^3}{24(1 - v_{FG}^2)} \end{pmatrix} \quad (16a)$$

$$\left(\frac{\partial^4 w}{\partial x^4} + 2\frac{\partial^4 w}{\partial x^2 \cdot \partial y^2} + \frac{\partial^4 w}{\partial y^4}\right) +$$

$$\begin{pmatrix} \frac{(\rho_c - \rho_m)h}{(k+1)} + \rho_m h \\ -(\rho_c + \rho_m)\frac{\beta h}{2} \end{pmatrix}\frac{\partial^2 w}{\partial t^2} = 0$$

$$\left(A \times \left(\frac{\pi}{a}\right)^4 + 2A \times \left(\frac{\pi}{a}\right)^2 \times \left(\frac{\pi}{b}\right)^2 + A \times \left(\frac{\pi}{b}\right)^4\right)$$

$$\times w(t) + \left(\frac{(\rho_c - \rho_m)h}{(k+1)} + \rho_m h - (\rho_c + \quad (16b)\right.$$

$$\left.\rho_m)\frac{\beta h}{2}\right)\frac{\partial^2 w(t)}{\partial t^2} = 0$$

where

$$A = \frac{(E_c - E_m)h^3}{(1 - v_{FG}^2)}$$

$$\left\{\frac{1}{k+3} - \frac{1}{k+2} + \frac{1}{4(k+1)}\right\} \quad (17)$$

$$+ \frac{E_m h^3}{12(1 - v_{FG}^2)} - \frac{(E_c + E_m)\beta h^3}{24(1 - v_{FG}^2)}$$

On solving, the following form was obtained as:

$$\omega_{mn}^2 w(t) + \frac{\partial^2 w(t)}{\partial t^2} = 0 \quad (18)$$

Then, the fundamental frequency can be given by,

$$\omega = \frac{\pi^2}{a^2}(1 + \gamma^2)\left(\frac{A(k+1)}{\rho_c h + \rho_m h - (k+1)(\rho_c + \rho_m)\frac{\beta h}{2}}\right)^{\frac{1}{2}} \quad (19)$$

where $\gamma = \frac{a}{b}$ is the aspect ratio. For a square plate, the natural frequency can be obtained as,

$$\omega = \frac{2\pi^2}{a^2}\left(\frac{A \times (k+1)}{h\left\{\rho_c + k\rho_m - (k+1)(\rho_c + \rho_m)\frac{\beta}{2}\right\}}\right)^{\frac{1}{2}} \quad (20)$$

where (ω) represents the natural frequency of the FG plate. The following formula can calculate the non-dimensional frequencies (ψ),

$$\psi = \frac{\omega L^2}{h}\sqrt{\frac{\int_{-h/2}^{h/2}\rho(z)\,dz}{\int_{-h/2}^{h/2}E(z)\,dz}} \quad (21)$$

In this work, the type of sandwich plate considered comprised of FGM core and homogeneous face sheets, as shown in Fig. 4,

and, in this case, the volume fraction of the FGM is taken as:

$$V_1(z) = V_{LP}, \qquad z \in [h_1, h_2]$$

$$V_c(z) = \left(\frac{z + \frac{h_{FG}}{2}}{h_{FG}}\right)^k, V_m = (1 - V_c), \; z \in [h_2, h_3] \quad (22)$$

$$V_3(z) = V_{UP}, \qquad z \in [h_3, h_4]$$

By assuming the skins are made from the same homogeneous materials, the mechanical properties $E_{UP} = E_{LP}, v_{UP} = v_{LP} = v$ and the mass density $\rho_{UP} = \rho_{LP}$; The general representation of the flexural rigidity and inertia of the sandwich plate (D_{SP} & I_{SP}) can be written as,

$$D_{SP}$$

$$= \begin{pmatrix} \int_{-\frac{(h_{FG}+h_{LP})}{2}}^{-\frac{(h_{FG})}{2}}\left(\frac{z^2}{(1 - v_{LP}^2)}E(z)\right)dz \\ + \frac{1}{(1 - v_{FG}^2)}\left(\int_{-\left(\frac{h_{FG}}{2}\right)}^{\left(\frac{h_{FG}}{2}\right)}\left(\begin{matrix} E_m + (E_c - E_m) \\ \left(\frac{z}{h} + \frac{1}{2}\right)^k - \\ (E_c + E_m)\frac{\beta}{2} \end{matrix}\right)z^2\right. \\ \left. dz\right) \\ + \int_{\left(\frac{h_{FG}}{2}\right)}^{\left(\frac{h_{FG}+h_{UP}}{2}\right)}\left(\frac{z^2}{(1 - v_{UP}^2)}E(z)\right)dz \end{pmatrix} \quad (23)$$

$$D_{SP}$$

$$= \frac{(E_c - E_m)h_{FG}^3}{(1 - v_{FG}^2)}\left\{\frac{1}{k+3} - \frac{1}{k+2}\right.$$

$$\left. + \frac{1}{4(k+1)}\right\} + \frac{E_m h_{FC}^3}{12(1 - v_{FG}^2)}$$

$$- \frac{(E_c + E_m)\beta h_{FG}^3}{24(1 - v_{FG}^2)} \quad (24)$$

$$+ \frac{E_{UP}}{(1 - v_{UP}^2)}\left(\frac{2\left(\frac{h_{FG}}{2} + h_{UP}\right)^3}{3} - \frac{h_{FG}^3}{12}\right)$$
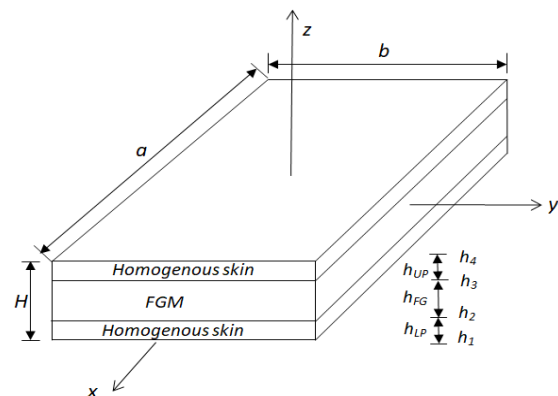

Fig. 4. PFGM rectangular sandwich plate geometry

And,

$$I_{SP} = \int_{-\frac{h}{2}}^{\frac{h}{2}} \rho(z)dz$$

$$= \left(\begin{array}{c} \int_{-\left(\frac{h_{FG}+h_{LP}}{2}\right)}^{-\left(\frac{h_{FG}}{2}\right)} \rho(z)dz + \\[2mm] \int_{-\left(\frac{h_{FG}}{2}\right)}^{\frac{h_{FG}}{2}} \left(\begin{array}{c} \rho_m + (\rho_c - \rho_m) \\ \left(\frac{z}{h} + \frac{1}{2}\right)^k \\ -(\rho_c + \rho_m)\frac{\beta}{2} \end{array} \right) dz \\[2mm] + \int_{\frac{h_{FG}}{2}}^{\left(\frac{h_{FG}+h_{UP}}{2}\right)} \rho(z)dz \end{array} \right) \quad (25a)$$

If, $h_{UP} = h_{LP}$, then get,

$$I_{SP} = \frac{(\rho_c - \rho_m)h_{FG}}{(k+1)} + \rho_m h_{FG}$$
$$-(\rho_c + \rho_m)\frac{\beta h_{FG}}{2} + 2\rho h_{UP}$$

$$I_{SP} = \frac{(\rho_c - \rho_m)h_{FG}}{(k+1)} + \rho_m h_{FG}$$
$$-(\rho_c + \rho_m)\frac{\beta h_{FG}}{2} + 2\rho h_{UP} \quad (25b)$$

The governing equation of plate now becomes (suppose m=n=1),

$$D_{sp}\left(\frac{\partial^4 w}{\partial x^4} + 2\frac{\partial^4 w}{\partial x^2 \cdot \partial y^2} + \frac{\partial^4 w}{\partial y^4}\right) + I_0\frac{\partial^2 w}{\partial t^2} = 0$$

$$D_{SP} = \left(\frac{\partial^4 w}{\partial x^4} + 2\frac{\partial^4 w}{\partial x^2 \cdot \partial y^2} + \frac{\partial^4 w}{\partial y^4}\right)$$
$$+ \left(\left(\frac{(\rho_c - \rho_m)h_{FG}}{(k+1)} + \rho_m h_{FG} - (\rho_c + \rho_m)\right)\frac{\beta}{2}h_{PG} + 2\rho h_{UP}\right)\frac{\partial^2 w}{\partial t^2} = 0 \quad (26)$$

FG sandwich plate with porous metal and Kirchhoff parallel plate, which are simply supported, can be related by equation (26). Using the comparison method, eq. (26) with a general equation of motion of SDF for free vibration of the structure.

When m = n = 1, one can find the fundamental vibration frequency. As a square plate has a square base, finding the fundamental natural frequency is straightforward.

$$\omega = 2\left(\frac{\pi}{a}\right)^2 \left\{ \frac{C(k+1)}{\begin{array}{c} \rho_c h_{FG} + k\rho_m h_{FG} \\ -(k+1)(\rho_c + \rho_m)\frac{\beta h_{FG}}{2} + \\ 2(k+1) \times \rho_{UP}h_{UP} \end{array}} \right\}^{1/2} \quad (27)$$

where

$$C = \left(\begin{array}{c} \frac{(E_c - E_m)h_{FG}^3}{(1 - v_{FG}^2)} \\[2mm] \left\{\frac{1}{k+3} - \frac{1}{k+2} + \frac{1}{4(k+1)}\right\} \\[2mm] + \frac{E_m h_{FG}^3}{12(1 - v_{FG}^2)} - \frac{(E_c + E_m)\beta h_{FG}^3}{24(1 - v_{FG}^2)} \\[2mm] + \frac{E_{UP}}{12(1 - v_{UP}^2)}\{(h_{FG} + 2h_{UP})^3 - h_{FG}^3\} \end{array} \right) \quad (28)$$

For convergence, the frequency parameter is:

$$\psi = \frac{\omega L^2}{h}\sqrt{\frac{\int_{-h/2}^{h/2} \rho(z)\,dz}{\int_{-h/2}^{h/2} E(z)\,dz}} \quad (29)$$

2.3. Numerical Investigation

By using finite element analysis, engineers can mathematically recreate the behavior of existing engineering systems. This means that the study must represent a physical prototype with an accurate mathematical model [51]. Numerical calculations are performed to determine the critical value of the natural frequency in which the ANSYS program provides stable performance in a sandwich plate structure made of FGM [52- 54]. Figure 1 illustrates the FG system employed in this analysis. SOLID186 elements with eight nodes are used to mesh the model as shown in Fig. 1. A mesh convergence test was performed to investigate the suitable mesh size to be used for carrying out the parametric studies. A comparison of sandwich flexural conductivity using functionally graded finite elements is carried out. Stipulations are linked between sandwich glue layers and between layers and skins to prevent genealogical development for each other at the connecting areas.

The numerical solution included drawing the structure after selecting the element types and then adding the mechanical properties of structural materials. As a part of loadings, the boundary condition was specified and no external forces were applied to perform the modal analysis. Because the free vibration analysis ignores all the forces and so the analysis reveals the internal characteristics of the system. The results of the present study were first compared with those published in the literature by solving general equations of motion for plate structures. This is done to determine if there is a discrepancy in the results calculated. This aligns with the analytical solution, indicating a sandwich plate structure with functionally graded material (FGM) cores and the influence of porosity.
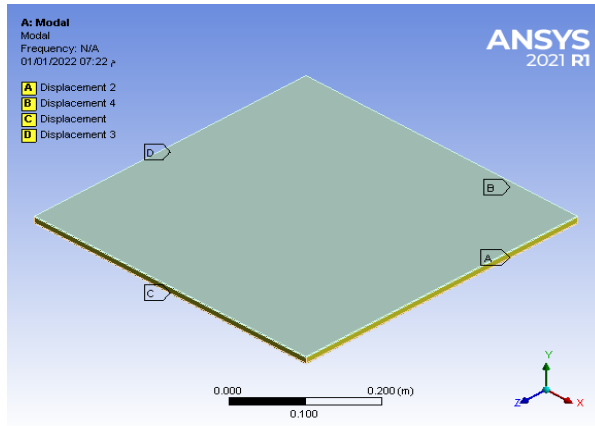
Fig. 5. The FG plate model with boundary conditions

Fig. 6. The mesh was created for the desired model

3. Results and Discussion

This work aims to analyze the free vibration analysis of an FG sandwich plate structure made of porous metal through an analytical approach. The results of the evaluation included the natural frequency and mode shapes of the simply supported FG sandwich plate with various parameters, such as the thickness of the FGM core, the thickness of the face sheet, and the aspect ratio. There are two types of plate parts, upper and lower, and ceramic and metals are considered in the FGM part. To verify the results, ANSYS software is used for numerical simulation, and multiple curves are drawn following the simulation. As shown in Table 1, FG plates and face sheets have a wide range of material characteristics. There are 4 dimensions of the plates a=b=0.5m, the power-law index k = (0, 0.5, 1, 2, and 5), and the porosity factor i = (0 to 0.4).

Table 1. Material properties of the (Al/Al$_2$O$_3$) FG sandwich plates

Property	FG plate		Face Sheets
	Aluminium (Al)	Ceramic (Al$_2$O$_3$)	
Young's modulus (GPa)	70	380	210
Mass density (kg/m³)	2702	3800	7800
Poisson's ratio	0.3	0.3	0.3

Tables 2, 3, and 4 present highly accurate Kirchhoff (classical thin) plate frequencies for various parameters such as aspect ratio, thickness ratios, and porous factor, these results are useful for examining convergence and accuracy. The frequency parameters can be calculated according to the following formula [54],

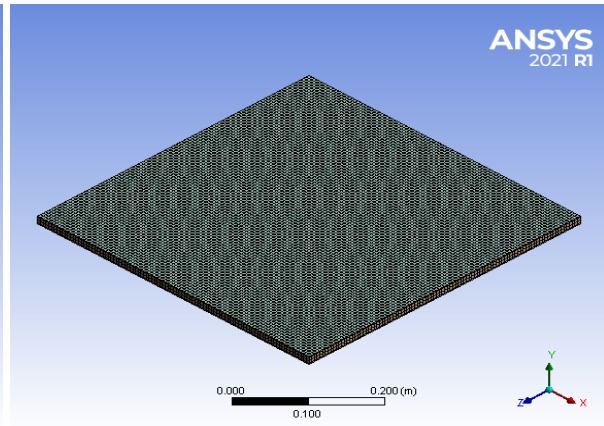$$\psi = \frac{\omega L^2}{h} \sqrt{\frac{\rho_o}{E_0}} \qquad (30)$$

where ω is the natural frequency, $\rho_o = 1$ kg/m³, $E_o = 1$ GPa

A mathematical model is described in Table 2 which predicts the natural frequency of square FGM sandwich plates without pores based on the same design and features of the sandwich plates. Slenderness ratios (a/h) of 10 and 100 as well as the volume fraction index (k) of 0 and 0.5 in addition to the current study results are used to assess previous studies.

Table 2. Comparisons of non-dimensional fundamental frequency parameters of imperfect FGM sandwich plates with different thickness ratios (*a/h*), porosity, and power-law exponents (*k*)

a/h	Ref.	k=0	k=0.5	k=1	k=5
10	[56]	1.8269	1.5768	1.4415	1.1757
	[25]	1.8269	1.5768	1.4415	1.1757
	[57]	1.8245	1.5746	1.4394	1.1740
	[58]	1.8242	1.5726	1.4371	1.1715
	Pres.	1.8205	1.5682	1.4280	1.1699
100	[56]	1.8884	1.6192	1.4756	1.1970
	[25]	1.8884	1.6192	1.4756	1.1970
	[57]	1.8883	1.6192	1.4756	1.1970
	[58]	1.8883	1.6192	1.4756	1.1970
	Pres.	1.8851	1.6177	1.4658	1.1676

Table 3, shows the results of the frequency parameter for four different aspect ratios, porous factors, and power-law indexes. It is noticed that increasing the grading indices decreases the natural frequency which improves the porous parameter due to the decreased material rigidity. In addition, as can be seen from Table 3, when frequency values are low (lower modes of frequency or thin plates), the analytical solution proposed by CPT is close to the proposed method, whereas, for higher mode

frequencies and higher plate thickness, CPT will have a larger error percentage.

It appears there is an apparent error of 25% between the numerical and analytical solutions at (a=10 h), which is dependent on the power-law index and porous factor.

The current analysis confirms the validity of the proposed approach. The impact of various boundary conditions such as CCCC, CCCS, CSCS, SSSS, and FCFC was studied and presented in Table 4. Out of these, the frequency is maximum for CCCC followed by CCCS, CSCS, SSSS, and FCFC. Also, the effects of the porous factor and gradient index were studied in which it was found that increasing the porosity fraction increases the natural frequency of an FG plate while the geometry parameter (k) increment reduces the natural frequency.

Table 3. The first nondimensional frequencies of square plates of (Al/Al$_2$O$_3$) are computed analytically and numerically for a wide range of power-law exponents (k) and porosity parameters (β)

		Power law index (k)											
		0		0.5		1		2		5		10	
a/h	Porosity	Ana.	Num.	Ana.	Num.	Ana.	Num.	Ana.	Num.	Ana.	Num.	Ana.	Num.
10	0	1.851	1.783	1.657	1.633	1.586	1.526	1.533	1.393	1.456	1.221	1.374	1.122
	0.1	1.872	1.804	1.666	1.644	1.589	1.528	1.530	1.382	1.445	1.187	1.353	1.071
	0.2	1.898	1.828	1.676	1.656	1.593	1.530	1.528	1.367	1.432	1.143	1.328	1.000
	0.5	2.004	1.927	1.723	1.713	1.610	1.638	1.516	1.292	1.365	1.268	1.187	1.137
20	0	1.855	1.836	1.689	1.704	1.630	1.612	1.588	1.502	1.527	1.366	1.463	1.291
	0.1	1.874	1.855	1.698	1.715	1.636	1.617	1.590	1.499	1.525	1.349	1.455	1.264
	0.2	1.895	1.876	1.709	1.728	1.643	1.623	1.593	1.494	1.522	1.327	1.445	1.227
	0.5	1.982	1.960	1.756	1.782	1.672	1.648	1.608	1.471	1.510	1.565	1.399	1.457
50	0	1.940	1.935	1.833	1.850	1.799	1.794	1.777	1.732	1.746	1.719	1.711	1.701
	0.1	1.957	1.952	1.846	1.864	1.812	1.806	1.789	1.741	1.757	1.724	1.720	1.709
	0.2	1.975	1.971	1.861	1.880	1.825	1.820	1.802	1.781	1.768	1.749	1.729	1.717
	0.5	2.044	2.038	1.916	1.937	1.876	1.869	1.850	1.840	1.812	1.793	1.767	1.749
100	0	2.201	2.208	2.198	2.188	2.135	2.129	2.129	2.128	2.118	2.120	2.102	2.078
	0.1	2.220	2.229	2.166	2.170	2.152	2.160	2.146	2.151	2.136	2.129	2.120	2.097
	0.2	2.239	2.241	2.185	2.176	2.171	2.180	2.166	2.149	2.155	2.090	2.139	2.112
	0.5	2.306	2.297	2.249	2.251	2.236	2.229	2.231	2.229	2.221	2.199	2.204	2.211

Table 4. The nondimensional fundamental frequency of square Al/Al$_2$O$_3$ Sandwich plates (face sheet thickness 2mm) with varying porosity factors, power-law indices, and BCs.

BC's	(k)	Porosity coefficient					
		0	0.1	0.2	0.3	0.4	0.5
CCCC	0	2.574	2.591	2.610	2.631	2.653	2.678
	0.5	2.435	2.446	2.457	2.469	2.481	2.494
	1	2.341	2.345	2.349	2.406	2.356	2.357
	2	2.227	2.223	2.217	2.255	2.197	2.178
	5	2.087	2.072	2.046	2.011	1.940	1.902
	10	2.009	1.981	1.938	1.839	1.826	1.814
CCCS	0	2.306	2.321	2.339	2.354	2.378	2.401
	0.5	2.183	2.193	2.204	2.216	2.229	2.243
	1	2.100	2.106	2.112	2.117	2.123	2.128
	2	2.003	2.003	2.001	1.998	1.993	1.985
	5	1.886	1.876	1.862	1.840	1.793	1.786
	10	1.823	1.805	1.777	1.707	1.705	1.705
CSCS	0	2.176	2.192	2.209	2.228	2.249	2.271
	0.5	2.065	2.076	2.088	2.101	2.116	2.131
	1	1.990	1.998	2.006	2.014	2.023	2.033
	2	1.904	1.907	1.909	1.911	1.911	1.910
	5	1.802	1.797	1.789	1.777	1.746	1.739
	10	1.747	1.736	1.719	1.669	1.659	1.652
SSSS	0	1.935	1.952	1.971	1.991	2.014	2.038
	0.5	1.850	1.864	1.880	1.897	1.916	1.937
	1	1.794	1.806	1.820	1.834	1.850	1.869
	2	1.731	1.741	1.751	1.762	1.774	1.787
	5	1.659	1.664	1.669	1.673	1.669	1.663
	10	1.621	1.623	1.531	1.606	1.599	1.589
FCFC	0	1.356	1.363	1.371	1.379	1.389	1.399
	0.5	1.274	1.277	1.280	1.284	1.288	1.291
	1	1.218	1.218	1.218	1.217	1.216	1.217
	2	1.153	1.148	1.143	1.136	1.127	1.116
	5	1.074	1.064	1.049	0.987	1.004	0.998
	10	1.031	1.015	0.995	0.959	0.949	0.940

Figures 7 and 8 demonstrate the analytical and numerical results of the frequency at β=0 and, k=0, for various FGM thicknesses. Increasing the FGM thickness increases the plate thickness thereby increasing the natural frequency. Also, it can be seen that beyond a certain value of grading index (k) no changes in the magnitude of frequency were seen.

The effect of various face sheet thicknesses (0.5, 0.75, 1, 2, and 2.5 mm) is presented in Figure 9. In contrast, in Fig. 10, the analytical results of the frequency at β=0 for various FGM thickness ratios are drawn, and it is concluded that the fundamental frequency increases with increasing porous factor. It is interesting to note that, here, beyond a/h=20, the change in frequency is insignificant.

Figure 11 presents a 3D surface plot illustrating the frequency parameter of a functionally graded square sandwich plate. This analysis was conducted using MATLAB code results for a porosity level (β = 0) and a face sheet thickness of 2 mm, across various power-law indices (k ranging from 0 to 100). Similarly, Figure 12 displays the plate's frequency

parameter at a porosity level of (β = 0.1). The findings show that the frequency parameter increases with higher porosity and geometrical properties due to the enhanced stiffness of the plate. Conversely, it decreases as the volume fraction index increases.

Figures 13 and 14 show analytical and numerical results for four values of aspect ratios (a/b = 0.75, 1, 1.5, and 2). The results show a good match with a maximum error percentage of 6 %.

In Fig. 15, the effect of the layer on the natural frequency for different aspect ratios of FGM rectangular plate at k = 0.5 and 5 with various thickness ratios was found. At the same time, Fig. 16 identifies the variation of the fundamental natural frequencies for different layers of FGM square plate layers at k = 0.5 for different thickness ratios; the figures show that there are no significant changes in the plate frequencies that occurred with increasing the layers, the reason may be due to the effective materials properties of the FG plate remains the same regardless the number of layers.
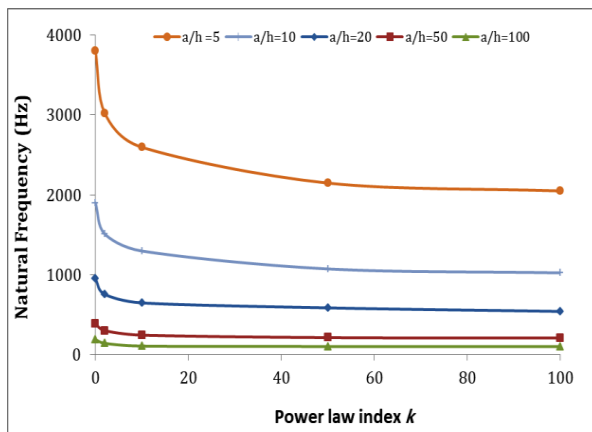

Fig. 7. Analytical results of the fundamental frequency at β=0
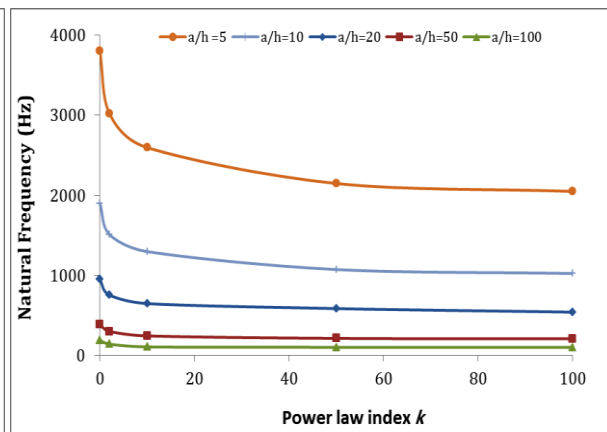

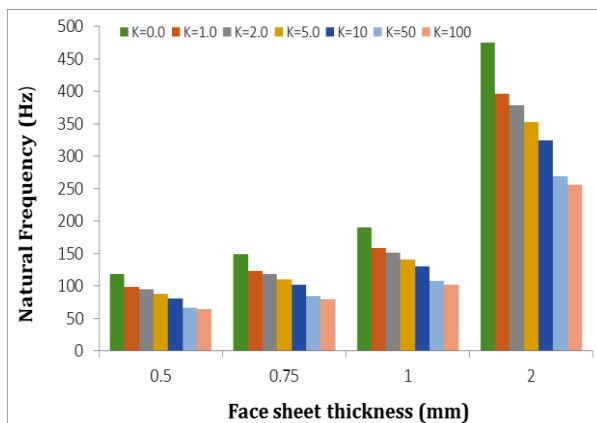**Fig. 8.** Numerical results of the fundamental frequency at β=0

Fig. 9. Analytical results of the fundamental frequency at β=0

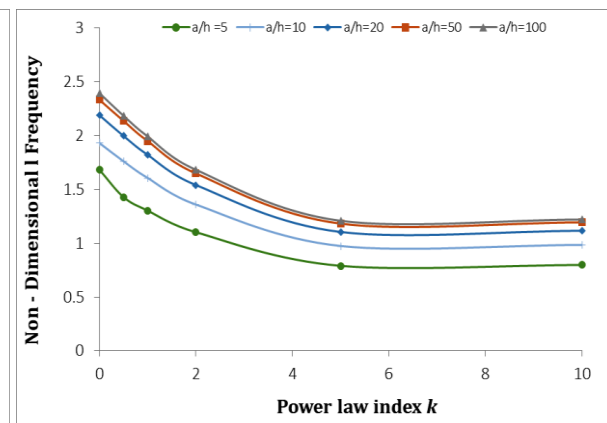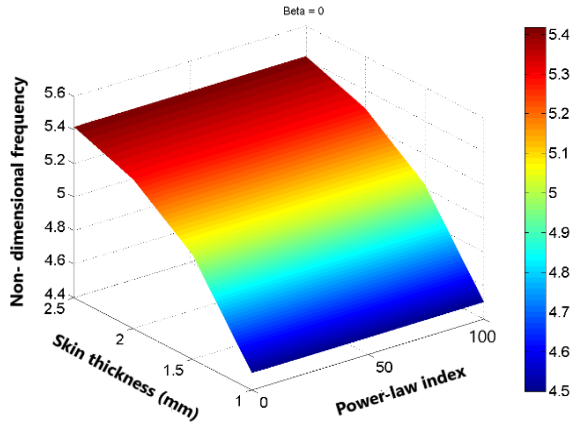**Fig. 10**. Analytical results of the fundamental frequency parameter at β=0

Fig. 11. Analytical natural frequency results at β=0 and k=0, for various FGM thicknesses
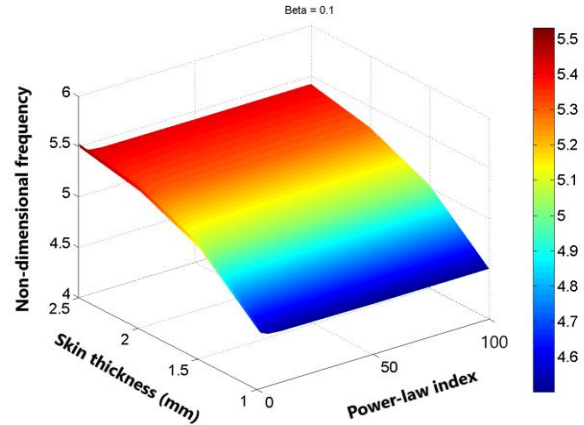

Fig. 12. Analytical results of the natural frequency at β=0
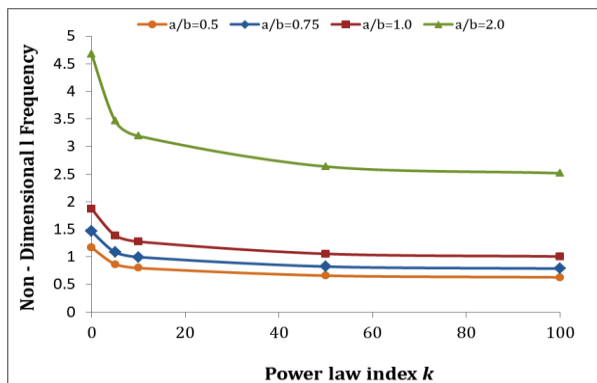

Fig. 13. Analytical results of the non-dimensional frequency of rectangular sandwich plates with various aspect ratios
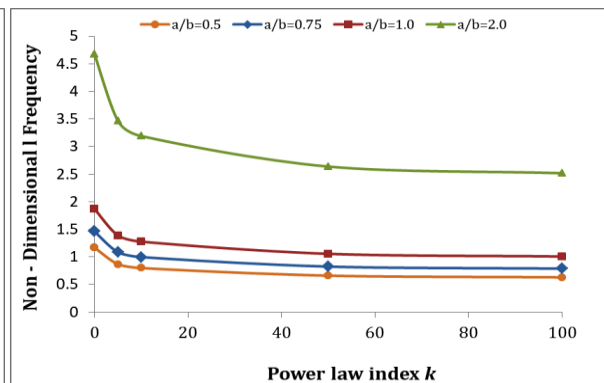

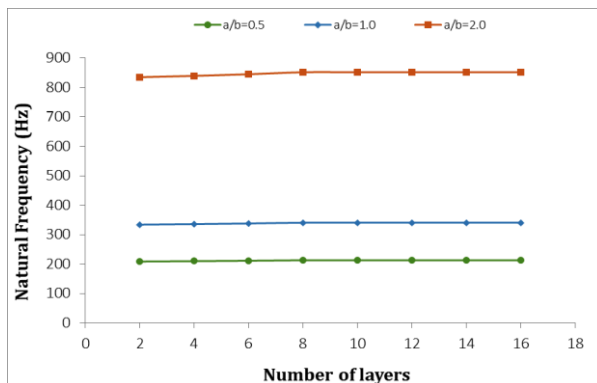**Fig. 14.** Numerical results of the non-dimensional frequency of rectangular sandwich plates with different aspect ratios

Fig. 15. The natural frequency of different numbers of layers of rectangular FGM plates at *k*=0.5
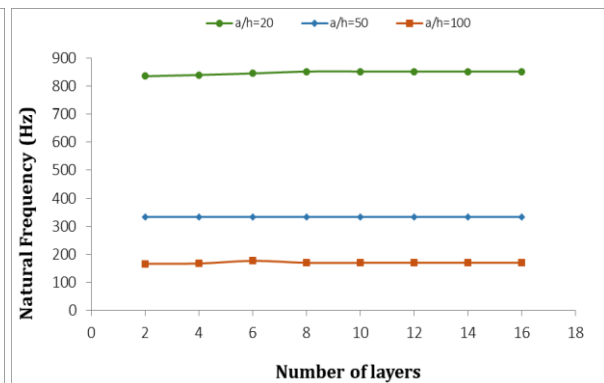

Fig. 16. The natural frequencies of FGM square plates for different numbers of layers at k = 0.5

4. Conclusions

The present study examines the free vibrations of the FGM sandwich plate, assuming that the material properties vary depending on the thickness with power distribution. Analytical solutions for free vibration analysis of simply supported plates are shown to demonstrate the accuracy of the proposed methodology. In the current study, the numerical results are obtained using ANSYS. Verification studies with some literature give accurate results for other plate theories for specific aspect ratio values and porous factors. Moreover, the exact relationship provides a practical way to check analytical results and software validity, convergence, and accuracy. From the above results, it can be concluded that:

1. Sandwich plates with a higher porous factor exhibit higher natural frequencies, while sandwich plates with a higher power-law index exhibit lower natural frequencies.

2. Analytical results and those obtained numerically are very closely aligned; the error percentages are not greater than 6%.

As the thickness ratio increases, the error will increase; for example, when the thickness ratio (a/h) is five, Kirchhoff's theory will produce an error of 22%.

3. Regardless of the layer thickness, the natural frequency of the FGM sandwich plate remains the same.

4. CCCC's frequency parameter is higher than CCCS's, and this condition is higher than CSCS's, etc., as shown in Table 4. The frequency parameter for CCCC increases with the restrictions to the boundary conditions.

Funding Statement

Conflicts of Interest

The author declares that there is no conflict of interest regarding the publication of this article.

References

[1] Suresh, S., & Mortensen, A., 1997. Functionally graded metals and metal-ceramic composites: Part 2 Thermomechanical behavior. *International Materials Reviews*, 42(3), pp. 85–116. https://doi.org/10.1179/imr.1997.42.3.85.

[2] Hadji L, Madan R, Bernard F., 2024. Thermal buckling in multi-directional porous plates: The effects of material grading and aspect ratio. *Proceedings of the Institution of Mechanical Engineers, Part G: Journal of Aerospace Engineering,* 238, pp. 412–426.

[3] Viet NV, Zaki W, Wang Q., 2020. Free vibration characteristics of sectioned unidirectional/bidirectional functionally graded material cantilever beams based on finite element analysis. *Applied Mathematics and Mechanics* (English Edition), 41, pp. 1787–1804.

[4] Saleh B, Jiang J, Fathi R, Al-hababi T, Xu Q, Wang L, Song D, Ma A., 2020. 30 Years of functionally graded materials: An overview of manufacturing methods, Applications and Future Challenges. *Composites Part B: Engineering,* 201, 108376.

[5] Matuła I, Dercz G, Barczyk J., 2020. Titanium/Zirconium functionally graded materials with porosity gradients for potential biomedical applications. *Materials Science and Technology,* 36, pp. 972–977.

[6] Khalili SMR, Nemati N., Malekzadeh K., Damanpack, AR., 2010. Free vibration analysis of sandwich beams using improved dynamic stiffness method. *Composite Structures,* 92, pp. 387–394.

[7] Mackerle J., 2002. Finite element analyses of sandwich structures: a bibliography (1980–2001). *Engineering Computations,* 19, pp. 206–245.

[8] Garg A, Chalak HD, Belarbi M-O, Zenkour AM., 2022. A parametric analysis of free vibration and bending behavior of sandwich beam containing an open-cell metal foam core. *Archives of Civil and Mechanical Engineering,* 22, 56.

[9] Chen C, Fang H, Zhu L, Han J, Li X, Qian Z., Zhang X., 2023. Low-velocity impact properties of foam-filled composite lattice sandwich beams: Experimental study and numerical simulation. *Composite Structures* 306, 116573.

[10] Cho J-R., 2022. Buckling analysis of sandwich plates with FG-CNTRC layers by natural element hierarchical models. *J Mech Sci Technol,* 36, pp. 1949–1957.

[11] Garg A, Chalak HD, Chakrabarti A., 2020. Comparative study on the bending of sandwich FGM beams made up of different material variation laws using refined layerwise theory. *Mechanics of Materials* 151, 103634.

[12] Chehel Amirani M., Khalili SMR, Nemati N., 2009. Free vibration analysis of sandwich beam with FG core using the element free Galerkin method. *Composite Structures* 90, pp. 373–379.

[13] Li D., Zhu H, Gong X., 2021. Buckling Analysis of Functionally Graded Sandwich Plates under Both Mechanical and Thermal Loads. *Materials,* 14, 7194.

[14] Naghavi M, Sarrami-Foroushani S, Azhari F., 2022. Bending analysis of functionally graded sandwich plates using the refined finite strip method. J*nl of Sandwich Structures & Materials,* 24, pp. 448–483.

[15] Pi Z., Zhou Z, Deng Z, Wang S., 2021. Bending and Buckling of Circular Sandwich Plates with a Hardened Core. *Materials,* 14, 4741.

[16] Vo TP, Thai H-T, Nguyen T-K, Maheri A, Lee J., 2014. Finite element model for vibration and buckling of functionally graded sandwich beams based on a refined shear deformation theory. *Engineering Structures,* 64, pp. 12–22

[17] Saidi H, Sahla M., 2019. Vibration analysis of functionally graded plates with porosity composed of a mixture of Aluminum (Al) and Alumina (Al2O3) embedded in an elastic medium. *Frattura ed Integrita Strutturale,* 13, pp. 286–299

[18] Merdaci S, Mostefa AH., 2019. Influence of porosity on the analysis of sandwich plates

FGM using of high order shear-deformation theory. *Fra&IntStrut,* 14, pp. 199–214

[19] Nguyen QH, Nguyen LB, Nguyen HB, Nguyen-Xuan H., 2020. A three-variable high order shear deformation theory for isogeometric free vibration, buckling and instability analysis of FG porous plates reinforced by graphene platelets. *Composite Structures,* 245, 112321.

[20] Yildirim S., 2020. Free Vibration Analysis of Sandwich Beams with Functionally-Graded-Cores by Complementary Functions Method. *AIAA Journal,* 58, pp. 5431–5439.

[21] Burlayenko VN, Sadowski T., 2020. Free vibrations and static analysis of functionally graded sandwich plates with three-dimensional finite elements. *Meccanica* 55, pp. 815–832.

[22] Al Rjoub YS, Alshatnawi JA., 2020. Free vibration of functionally-graded porous cracked plates. *Structures, 2*8, pp. 2392–2403.

[23] Kumar V, Singh SJ, Saran VH, Harsha SP., 2021. Vibration characteristics of porous FGM plate with variable thickness resting on Pasternak's foundation. *European Journal of Mechanics - A/Solids,* 85, 104124.

[24] Wang Q, Li Z, Qin B, Zhong R, Zhai Z., 2021. Vibration characteristics of functionally graded corrugated plates by using differential quadrature finite element method. *Composite Structures,* 274, 114344.

[25] Ganapathi M., Makhecha DP., 2001. Free vibration analysis of multi-layered composite laminates based on an accurate higher-order theory. *Composites Part B: Engineering,* 32, pp. 535–543.

[26] Ye W, Liu J, Zhang J, Yang F, Lin G., 2021. A new semi-analytical solution of bending, buckling and free vibration of functionally graded plates using scaled boundary finite element method. *Thin-Walled Structures,* 163, 107776.

[27] Sitli Y, Mhada K, Bourihane O, Rhanim H., 2021. Buckling and post-buckling analysis of a functionally graded material (FGM) plate by the Asymptotic Numerical Method. *Structures*, 31, pp.1031–1040.

[28] Bui TQ., Nguyen MN., 2011. A novel meshfree model for buckling and vibration analysis of rectangular orthotropic plates. *Structural Engineering and Mechanics,* 39, pp. 579–598

[29] Yang Y, Lam CC, Kou KP, Iu VP., 2014. Free vibration analysis of the functionally graded sandwich beams by a meshfree boundary-domain integral equation method. *Composite Structures,* 117, pp. 32–39.

[30] Kumar R, Sharma HK, Gupta S, Malguri A., Rajak B., Srivastava Y., Khan S., Pandey A., 2024. Initial Buckling Behavior of Elastically Supported Rectangular FGM Plate based on Higher Order Shear Deformation Theory via Spline RBF Method. *Mechanics of Advanced Composite Structures,* 11, pp. 59–72.

[31] Tossapanon P., Wattanasakulpong N., 2016. Stability and free vibration of functionally graded sandwich beams resting on two-parameter elastic foundation. *Composite Structures,* 142, pp. 215–225.

[32] Xue Y., Jin G, Ma X, Chen H, Ye T, Chen M., Zhang Y., 2019. Free vibration analysis of porous plates with porosity distributions in the thickness and in-plane directions using isogeometric approach. *International Journal of Mechanical Sciences,* 152, pp. 346–362.

[33] Madan R, Bhowmick S., 2020. A review on application of FGM fabricated using solid-state processes. *Advances in Materials and Processing Technologies,* 6, pp. 608–619.

[34] Mohammadi M, Rajabi M, Ghadiri M., 2021. Functionally graded materials (FGMs): A review of classifications, fabrication methods and their applications. *Processing and Application of Ceramics,* 15, pp. 319–343.

[35] Madan R, Bhowmick S., 2022. Fabrication, microstructural characterization and finite element analysis of functionally graded Al-Al2O3 disk using powder metallurgy technique. *Materials Today Communications,* 32, 103878.

[36] Madan R., Bhowmick S., 2022. Fabrication, Microstructural Characterization and Finite Element Analysis of Functionally Graded Al-Al2O3 Disk Using Powder Metallurgy Technique. *Materials Today Communications,* 103878.

[37] Ansari M., Jabari E., Toyserkani E., 2021. Opportunities and challenges in additive manufacturing of functionally graded metallic materials via powder-fed laser directed energy deposition: A review. *Journal of Materials Processing Technology* 294, 117117.

[38] Bobbio LD, Bocklund B, Simsek E, Ott RT, Kramer MJ, Liu Z-K, Beese AM., 2022. Design of an additively manufactured functionally graded material of 316 stainless steel and Ti-6Al-4V with Ni-20Cr, Cr, and V intermediate compositions. *Additive Manufacturing.* https://doi.org/10.1016/j.addma.2022.102649

[39] Alkunte S., Fidan I., Naikwadi V., Gudavasov S., Ali MA, Mahmudov M., Hasanov S., Cheepu M., 2024. Advancements and Challenges in Additively Manufactured Functionally Graded Materials: A

Comprehensive Review. *Journal of Manufacturing and Materials Processing.* https://doi.org/10.3390/jmmp8010023

[40] Wang S., Duan G., 2024. Process parameter modeling for the fabrication of functionally graded materials via direct ink writing. *The International Journal of Advanced Manufacturing Technology,* 132, pp. 3415–3426.

[41] Chen W, Wang Q, Zai C, Ma C, Zhu Y, He W., 2001. Functionally graded Zn-Al-Si in-situ composites fabricated by centrifugal casting. *Journal of Materials Science Letters,* 20, pp. 823–826

[42] Zygmuntowicz J, Wiecińska P, Miazga A, Konopka K, Kaszuwara W., 2017. Al2O3/Ni functionally graded materials (FGM) obtained by centrifugal-slip casting method. *Journal of Thermal Analysis and Calorimetry,* 130, pp. 123–130.

[43] Jamian S, Ayob SN, Abidin MRZ, Muhd Nor NH., 2016. Fabrication of functionally graded natural fibre/epoxy cylinder using centrifugal casting method. *ARPN Journal* of Engineering and Applied Sciences, 11, pp. 2327–2331.

[44] Avcar M, Hadji L, Civalek Ö., 2023. Free vibration analysis of porous functionally graded sandwich beams. In: Functionally Graded Structures. *IOP Publishing*, pp 8–1.

[45] Avcar M, Hadji L, Tounsi A., 2023. The static bending analysis of porous functionally graded sandwich beams. *Functionally Graded Structures,* 4–1 to 4–17

[46] Ghazwani MH, Alnujaie A, Avcar M, Van Vinh P., 2024. Examination of the high-frequency behavior of functionally graded porous nanobeams using nonlocal simple higher-order shear deformation theory. *Acta Mechanica,* 235, pp. 2695–2714.

[47] Hadji L, Avcar M., 2020. Free Vibration Analysis of FG Porous Sandwich Plates under Various Boundary Conditions. *J. Appl. Comput. Mech.,* https://doi.org/10.22055/jacm.2020.3532 8.2628

[48] Koutoati K, Mohri F, Daya EM, Carrera E., 2021. A finite element approach for the static and vibration analyses of functionally graded material viscoelastic sandwich beams with nonlinear material behavior. *Composite Structures,* 274, 114315.

[49] Zghal S, Dammak F., 2021. Vibration characteristics of plates and shells with functionally graded pores imperfections using an enhanced finite shell element. *Computers & Mathematics with Applications*, 99, pp. 52–72.

[50] Raad H., Najim E., Jweeg M, AlWaily M., Hadji L, Madan R., 2024. Vibration Analysis

of Sandwich Plates with Hybrid Composite Cores Combining Porous Polymer and Foam Structures. *JCAM*. https://doi.org/10.22059/jcamech.2024.37 7658.1121

[51] Jebur, Q. H., Hamzah, M. N., Jweeg, M. J., Njim, E. K., Al-Waily, M., & Resan, K. K., 2024. Modeling hyperplastic elastomer materials used in tire compounds: numerical and experimental study. In Journal Teknologi, 86 (5), pp. 77–87. *Penerbit UTM Press.* https://doi.org/10.11113/jurnalteknologi.v 86.21003

[52] Mouthanna, A., Bakhy, S. H., Al-Waily, M. and Njim, E. K., 2023. Free Vibration Investigation of Single-Phase Porous FG Sandwich Cylindrical Shells: Analytical, Numerical and Experimental Study. Iranian Journal of Science and Technology, *Transactions of Mechanical Engineering.* Springer Science and Business Media LLC, Aug. 29, https://doi.org/10.1007/s40997-023-00700-7

[53] Neamah, R. A., Al-Raheem, S. K., Njim, E. K., Abboud, Z., & Al-Ansari, L. S., 2024. Experimental and Numerical Investigation of the Natural Frequency for the Intact and Cracked Laminated Composite Beam*. In Journal of Aerospace Technology and Management, 16. FapUNIFESP (SciELO). https://doi.org/10.1590/jatm.v16.1337*

[54] Njim E.K., Hasan H.R., Jweeg MJ, Al-Waily M, Hameed A.A., Youssef A.M., Elsayed F.M., 2024. Mechanical Properties of Sandwiched Construction with Composite and Hybrid Core Structure. *Advances in Polymer Technology,* 2024, 3803199.

[55] Van Vinh P., Huy LQ., 2022. Finite element analysis of functionally graded sandwich plates with porosity via a new hyperbolic shear deformation theory. *Defence Technology,* 18, pp. 490–508.

[56] Li Q., Iu VP, Kou KP., 2008. Three-dimensional vibration analysis of functionally graded material sandwich plates. *Journal of Sound and Vibration, 311, pp. 498–515*

[57] Zenkour AM., 2005. A comprehensive analysis of functionally graded sandwich plates: Part 1—Deflection and stresses. *International Journal of Solids and Structures,* 42, pp. 5224–5242.

[58] Zenkour AM., 2005. A comprehensive analysis of functionally graded sandwich plates: Part 2—Buckling and free vibration. *International Journal of Solids and Structures,* 42, pp. 5243–5258.